Monolithic integrated InGaAsP/InP distributed feedback laser with Y-branching waveguide and a monitoring photodetector grown by metalorganic chemical vapor deposition

K.-Y. Liou, U. Koren,[a] S. Chandrasekhar,[b] T. L. Koch,[a] A. Shahar,[a] C. A. Burrus, and R. P. Gnall[a]

AT&T Bell Laboratories, Crawford Hill Laboratory, Holmdel, New Jersey 07733

(Received 12 September 1988; accepted for publication 25 October 1988)

We have fabricated an integrated 1.5 μm distributed feedback laser (DFB) with a Y-branching waveguide and a monitoring photodetector, grown entirely by metalorganic chemical vapor deposition. The integrated device is designed to resolve the frontface-backface mistracking problem of the DFB laser and to demonstrate monolithic integration of fundamental building blocks for photonic integrated circuits.

Photonic integrated circuits (PICs), consisting of active and passive optical components fabricated on a single III-V semiconductor substrate, are potentially important for lightwave technologies. We describe in this letter the monolithic integration of a single-mode distributed feedback (DFB) laser, a Y-branching waveguide, and a monitoring photodetector. This DFB-Y-detector PIC resolves the frontface-backface output mistracking problem of the DFB laser and can significantly simplify laser packaging in the future. The PIC wafer was grown entirely by metalorganic chemical vapor deposition (MOCVD).

When a semiconductor laser is used in optical fiber communication systems, the frontface output power is monitored by a backface output detector. This method, conventionally used for a Fabry–Perot laser, cannot be applied to a DFB laser. The outputs from two sides of a DFB laser with randomly cleaved facets can differ by a factor as large as 2,[1,2] and the ratio may change as the laser degrades. This DFB frontface-backface mistracking problem is caused by the light phase effect of grating reflection relative to facet reflection that varies the external differential efficiency. Also, in the case when one facet of a DFB laser is destroyed to suppress the Fabry–Perot resonances, the outputs from the two sides are completely different. A frontface detector is integrated in our device to resolve this problem. Furthermore, the two-mode degeneracy of an axially symmetric DFB laser[3] is removed with the asymmetric reflectivity configuration of the integrated DFB laser, resulting in stabilized single DFB mode oscillation.

The DFB-Y-detector PIC is shown schematically in Fig. 1. The laser is a semi-insulating planar buried heterostructure (SIPBH) type[4] with a first-order grating. The emission wavelength is near 1.5 μm. The laser oscillates in the fundamental mode, which is coupled to the adjacent 1.3 μm passive waveguide layer,and the output is guided by the Y-branching waveguide. A symmetrical Y junction is integrated as a 3 dB power divider. "S"-shaped bends are employed to reduce the bending loss. The radius of the curved sections of the S bends equals 11.7 mm. A taper length of 100 μm is used for the input straight section of the Y junction. The branching angle between the two tangent lines at the splitting point is 2°. One of the two branches is used as the output port and the other is coupled to an integrated *p-i-n*-detector. The same laser structure without the grating is used for the detector. The passive waveguide is buried in semi-insulating InP, which has a smaller absorption loss coefficient than *p*-InP. Figure 2 shows the details of longitudinal cross-sections of the laser and the output ends. The 200-Å-thick stop-etch layers, which are important for PIC processing but have insignificant effect on waveguiding, are not shown in Figure 2. Both the laser and the detector are 250 μm long and the total length of the PIC is 2540 μm.

The PIC fabrication involves the following steps. First, seven layers are grown by MOCVD on an *n*-InP substrate. These layers are a 200-Å-thick InGaAsP stop-etch layer, a 1.6-μm-thick *n*-InP cladding layer, a 2700 Å InGaAsP ($\lambda \sim 1.3\,\mu$m) passive waveguide layer, a 200 Å InP stop-etch layer, a 1000 Å undoped InGaAsP ($\lambda \sim 1.5\,\mu$m) active layer, a 1500 Å InGaAsP ($\lambda \sim 1.3\,\mu$m) waveguide layer, and a 1200 Å *p*-InP layer. The top *p*-InP layer, except for the detector areas, is then removed by wet chemical etching. Then, a first-order holographic grating is produced everywhere on

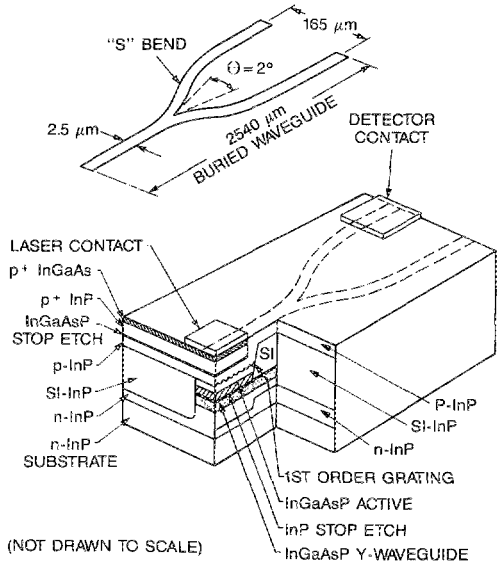

FIG. 1. Schematic diagram of the DFB-Y-detector PIC. The location of the buried waveguide is shown projected on the top surface by dotted lines.

[a] AT&T Bell Laboratory, NJ 07733.

[b] On leave from the Tata Institute of Fundamental Research, Bombay, India.

 0003-6951/89/020114-03$01.00

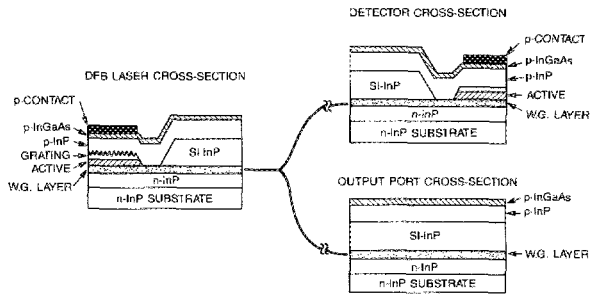

FIG. 2. Longitudinal cross sections of the laser end, the detector end, and the waveguide output port.

the wafer. By selectively etching away the p-InP layer on the detector areas and then etching off the InGaAsP layers on top of the InP stop-etch layer in the passive waveguide areas, the grating is left only on the laser areas while the active layer is left on both the laser and detector areas. The Y-waveguide mesa is etched using a SiO_2 mask with the straight sections parallel to the (011) orientation, followed by a MOCVD regrowth of Fe-doped semi-insulating (SI) InP layer for current blocking and lateral optical confinement. It is important to note that a shallow etch is done for the passive waveguide and a deep etch for the laser and detector. Also, the SiO_2 mask is removed from the region of the passive waveguide before the regrowth. Therefore, after the regrowth, the long passive waveguide is buried in the low-loss SI InP layer, as illustrated in Figs. 1 and 2. This is followed by removing the remaining SiO_2 mask and then a second MOCVD regrowth of a p-InP layer, an InGaAsP stop-etch layer, a p^+-InP layer, and a p^+-InGaAs cap layer. The stop-etch layer is used to remove part of the conducting p layers to increase the electrical isolation between the laser and the detector. All the wet etching steps above are done using the standard selective etchants—a 2:1 mixture of $HCl:H_3PO_4$ for InP and a 3:1:1 mixture of $H_2SO_4:H_2O_2:H_2O$ for InGaAsP and InGaAs. Finally, standard metallization is applied to the lasers and detectors for electrical contacts. The PIC chips are cleaved from the wafer and are mounted p-side up on copper studs.

Single DFB mode and fundamental transverse mode oscillation of the laser, Y-junction power coupling, and a high detector photocurrent were all demonstrated. Figure 3 shows, for one PIC sample, the photocurrent of the integrated detector versus the laser injection current at 25 °C. The photocurrent was recorded with the detector unbiased. The output powers from both the laser side and the Y-branch output port of the PIC chip, measured with an external photodiode, are also shown as dashed lines in the figure. With cleaved facets on both ends, the total power from the Y-branch output side is close to one half of the output from the laser side for this sample. The detector photocurrent is about 150 μA/mW power from the Y-branch output port. Some small kinks on the output light-current curves a and b, caused by reflections from the cleaved facets, are clearly reproduced on the monitoring photocurrent curve. Single DFB mode output was observed for injection currents from 35 mA, the laser threshold, to 150 mA with a 32 dB side-mode suppression.

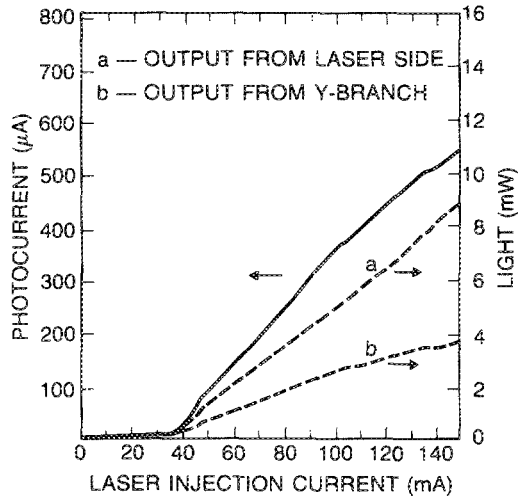

FIG. 3. Detector photocurrent vs laser injection current of a PIC sample measured at 25 °C with the detector unbiased. The PIC has cleaved facets on both sides. The output light powers measured with an external power meter are shown as dashed curves.

The electrical isolation between the laser and the detector of the finished chips is in the range of 1–10 MΩ. A good electrical isolation is important for an integrated detector, because the leakage current from the laser bias to the detector is added to the reverse dark current of the detector in the external circuit. With a typical 0.5 V turn-on voltage for a laser diode, the leakage current to the detector due to laser bias is less than 0.5 μA for isolation greater than 1 MΩ. The measured detector dark currents at 22 °C with the laser unbiased are plotted as a function of detector reverse voltage in Fig. 4 for two typical integrated detectors. Since a reverse bias is not necessary when the integrated detector is used to monitor the average laser output power, Fig. 4 shows that the dark current is negligible compared to the photocurrent.

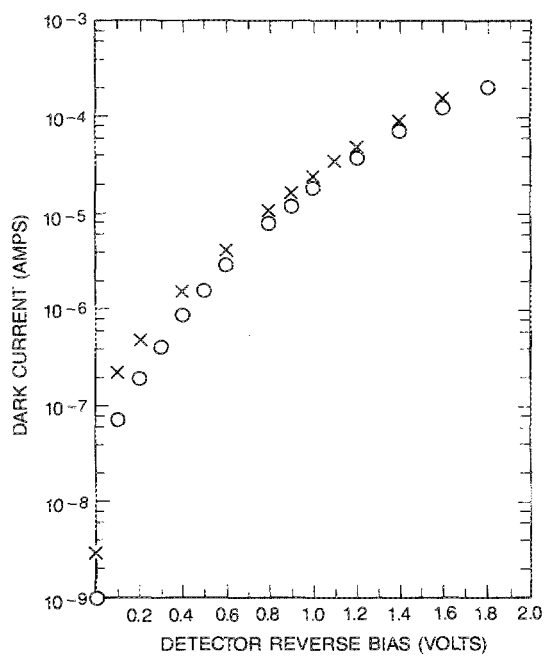

FIG. 4. Reverse dark currents of the integrated detector at 22 °C for two typical PIC samples.

To estimate the Y-branching loss and the detector efficiency, straight waveguides with an integrated DFB laser on one end and a detector on the other were fabricated on the same wafer with the Y-waveguide devices. The waveguide propagation loss, measured separately using straight waveguides without the integrated laser and detector, is about 3 dB/cm. This was determined from the attenuation of light propagating in straight waveguide samples of known lengths. Very similar photocurrents, 140 to 150 μA/mW power from the Y-output port, were measured for all DFB-Y-detector PIC samples. By comparing the photocurrents of the Y waveguide and straight waveguide devices at a same output power from the laser facet side, the Y-branching loss can be estimated.

In addition to the 3 dB branching loss, an excess Y-junction loss of about 3 dB was determined for the best samples. Waveguide taper, mode mismatch, and waveguide bend contribute to the Y-junction loss. The observed 3 dB excess loss was verified by calculations to be due mainly to a blunted wedge tip found between the two branching waveguides at the Y-junction. In our case, the blunting was caused by the stepped wall of the computer designed mask for the waveguide bend and wet etching under cut, both can be modified to reduce the excess loss. An excess loss of less than 1 dB has been reported previously for a discrete semiconductor Y junction,[5] indicating that low-loss Y junctions can be fabricated for PIC applications.

Since a sufficiently large monitoring photocurrent has been obtained, the symmetrical Y junction can be replaced in the future with a directional coupler or an asymmetrical Y junction with less than 3 dB power coupling to the detector. A low-reflectivity coating on the output facet and a high-reflectivity coating on the DFB laser side will also increase the waveguide output power for use in optical fiber transmission systems.

In conclusion, we have fabricated a DFB-Y-detector PIC with stable single-mode light output monitored by an integrated detector. The PIC resolves the DFB frontface-backface mistracking problem and may simplify laser packaging. A very good electrical isolation, higher than 1 MΩ between the laser and the detector, was achieved without affecting the performance of the single-mode buried waveguide. The results demonstrate the capability of monolithic integration of fundamental PIC building blocks—laser, detector, passive waveguide, power coupler, and corrugation grating—using our MOCVD growth and processing techniques.

We thank E. C. Burrows for technical assistance and M. A. Pollack for support and encouragement.

[1]T. Matsuoka, Y. Yoshikuni, and H. Nagai, IEEE J. Quantum Electron. **QE-21**, 1880 (1985).
[2]G. P. Agrawal, N. K. Dutta, and P. J. Anthony, Appl. Phys. Lett. **48**, 457 (1986).
[3]H. Kogelnik and C. V. Shank, J. Appl. Phys. **43**, 2327 (1972).
[4]U. Koren, B. I. Miller, G. Eisenstein, G. Raybon, and R. J. Capik, Electron. Lett. **24**, 138 (1988).
[5]L. M. Johnson, Z. L. Liau, and S. H. Groves, Appl. Phys. Lett. **44**, 278 (1984).